CONF-9604105--2

LA-UR- 96-834

Title: Directional Wind-Measurement Derived from Elastic Backscatter Lidar Data in Real-Time

Author(s): David S. Moore, Stephen W. White, Robert R. Karl, Jr., and Brian E. Newnam

Submitted to: SPIE Aerosense '96, Orlando, FL, April 1996

Los Alamos
NATIONAL LABORATORY

Directional Wind-Measurement Derived From Elastic Backscatter Lidar Data In Real-Time

D.S. Moore, S.W. White, R.R. Karl, Jr., and B.E. Newnam

Los Alamos National Laboratory, Los Alamos NM 87544

ABSTRACT

The development of a capability to infer wind velocities simultaneously at a number of ranges along one direction in real time is described. The elastic backscatter lidar data used was obtained using the XM94 lidar, developed by Los Alamos National Laboratory for the US Army Chemical and Biological Detection Command. In some respects this problem is simpler than measuring wind velocities on meso-meteorological scales. Other requirements, particularly high temporal fidelity, have driven the development of faster software algorithms and suggested opportunities for the evolution of the hardware.

1. INTRODUCTION

The incoherent aerosol lidar technique of Prof. E. Eloranta of the University of Wisconsin has been used to measure winds on meso-scales meteorology.[1] The same methodology can be adapted to obtain two dimensional wind information near the ground in real time. For this purpose, an elastic back scattering lidar (light-detection-and-ranging) technique for observing aerosol patterns moving with the wind was used. The goal of this work was to process in real time (less than one second) the detected lidar signals to yield wind velocity using a fast computer algorithm adapted from the meso-scale methodology. Success in this effort was verified using both simulated patterns of aerosols and real lidar data.

2. EXPERIMENT AND THEORY

To facilitate development of the wind velocity calculation algorithm, elastic back scattering lidar data was obtained using the Los Alamos XM94 near infrared lidar system. Data was obtained in field tests at four different locations – Los Alamos, Aberdeen Proving Grounds (APG), White Sands Missile Range (WSMR), and Dugway Proving Grounds (DPG). Aerosol patterns moving with the wind at ranges from 100 m to 10 km were detected. As expected, lidar scattering from the aerosols was most evident at sea level and decreased with altitude (up to 7000 feet). During the development of the wind measurement algorithm, this data was stored and analyzed off-line.

The XM94 lidar system has the following specifications:

Wavelength:	1064 nm
Pulse width:	6 ns FWHM
Energy/pulse:	200-400 mJ
Repetition rate:	20 Hz
Beam divergence:	0.5 mr full angle
Collector diameter:	20 inches
Telescope sweep rates:	0.1°/sec to 10°/sec
Detector:	Si APD, 8 MHz
Computer on-line:	Sun Sparc 20
Digitizer:	VME 25 MHz

Real-time display of backscatter signal versus range
Real-time 2-D color-enhanced display of backscatter signals

MOORE

There are a variety of atmospheric properties that can affect lidar cross-wind measurements. Aerosols are most dense at low altitudes, but are very dilute at higher elevation or in dry climates. Turbulent mixing decreases persistence and size of the aerosol structures near the ground. Rough correlations can be made between aerosol structure size and persistence time with their height above the ground surface.[2] It is also known that the aerosol distribution varies with the time of day and with terrain (because of pollens, dust and moisture). The relatively slow detector circuit used in the XM94 (see above) effectively diminishes the aerosol backscattering signal contrast via temporal convolution. At near-surface observation heights of about 2 m, the dominant aerosol dimension is approximately also 2 m. The detector used, however, was only able to resolve features of the order of 10 m size. Thus, the present system measured the motion of larger aerosol patterns that also have correspondingly longer persistence times. More information about smaller aerosol patterns, which are probably more numerous and have shorter persistence times, will require a faster detector and a correspondingly faster digitizer (discussed further below).

The algorithm is largely a subset of the work described by Schols and Eloranta.[1] The first step in the process utilized here involves binning the lidar scan data into 12 range-resolved segments of 16 x 16 bins each. The factor 16 was chosen to be a power of two, to provide reasonable spatial resolution commensurate with the time resolution of the lidar system, and to result in adequate calculation speed for the algorithm.

After binning, a histogram equalization routine[1] was used to sharpen the contrast in the scan images. The scan data, which can be represented as a distribution of pixel brightness values, can be dominated by anomalously bright targets which bias the measured average velocity to the velocity of the brightest targets. To reduce this effect, the pixel brightness distribution was made uniform by changing pixel brightness values according to the transformation:

$$f_u(\mathbf{x},t) = P\left[f^f(\mathbf{x},t))\right]$$

where $f_u(\mathbf{x},t)$ corresponds to the new pixel brightness distribution and P stands for the cumulative probability distribution of the initial pixel brightness distribution. In effect, pixel brightness values that lie in the tails of the distribution are compressed, whereas the pixel brightness values in the central region are expanded.

The lidar images may also contain structures that do not move with the wind, such as telephone poles, buildings, and atmospheric features which are anchored to the underlying terrain,. To remove these features, a temporal median filter at each range is constructed over a time interval centered about each image:

$$f^m(\mathbf{x},t_i) = \text{median}\left[f\left(\mathbf{x},t_j\right)\right] \quad \text{for i-}l \le \text{j} \le \text{i+}l$$

where $f\left(\mathbf{x},t_j\right)$ is the instantaneous aerosol backscattering distribution in an image at time t_i and at grid location $\mathbf{x} = (x,y)$, and $2l$ is the width of the temporal median. The median image is then subtracted from each subsequent scan, and is also continuously updated by each subsequent scan, to obtain the temporal high pass median filtered image

$$f^f(\mathbf{x},t_i) = f(\mathbf{x},t_i) - f^m(\mathbf{x},t_i)$$

Ideally, the median image is computed over a time period that is short compared to the rate at which the stationary background image changes, yet long enough that many wind driven aerosol structures pass over

each image point. For these studies of cross-wind measurements close to the ground, five scans were used.

2.1 Spatial Cross Correlation Calculations

The location of the maximum value of the two-dimensional spatial cross correlation function (CCF) was used to estimate the motion of aerosol structures. The value of this function between patterns $f_u(\mathbf{x},t_1)$ and $f_u(\mathbf{x},t_2)$ observed at successive times t_1 and t_2, respectively, is given by:

$$C(\delta\mathbf{x},t_1,t_2-t_1)=\int_S f_u(\mathbf{x},t_1)\, f_u(\mathbf{x}+\delta\mathbf{x},t_2)\,\mathrm{d}S$$

where $\delta\mathbf{x} = (\delta x, \delta y)$ is a lag vector and the integral is taken over the surface S of each range segment.

The CCF function is efficiently evaluated using two dimensional discrete Fourier transforms (DFT's) and is proportional to:

$$F^{-1}\left(F^{*}\left(f_u(\mathbf{x},t_1)\right)\bullet F\left(f_u(\mathbf{x},t_2)\right)\right)$$

where F is the forward transform, F^{-1} is the inverse DFT, * denotes the complex conjugate and the product is pairwise multiplication of the two dimensional arrays.

The largest value in the amplitude of the cross correlation matrix is used to locate the peak correlation. Inverse quadratic interpolations in both directions provide the spatial displacement of the strongest correlated feature between the two frames. These computations, which have been made in the original polar coordinates, are now transformed into Cartesian coordinates. The time interval between frames and the Cartesian displacements yields the crosswind and range wind velocities for each segment.

At this point we have calculated values of the wind velocities and the magnitude of the correlation. These numbers do contain statistical errors, but rather than smoothing them by temporal averaging, we decided to accept them provided the correlation exceeded an experimentally determined threshold. In the cases where the threshold was not met we multiplied the previous velocities by a number less than or equal to 1. This permits a gradual diminishing of the calculated velocities until another strong correlation comes along.

Along with the mathematical algorithm, we developed a sensible display of the range-resolved calculated wind speeds to accompany the standard XM94 lidar system display. The wind display shows the calculated wind velocities within one hundred meter range increments and borrows from standard meteorological wind indicator conventions. Each range increment is displayed as a circle, within which an arrow that points into the wind is located. The tail feathers on the arrow are sized in proportion to the wind velocity at that range. The color of each arrow is an indication of the strength of the correlation (i.e. the confidence in the calculation) following the rainbow colors with red being highest.

3. RESULTS

After development, the algorithm was coded, installed on the XM94, and field tested at Los Alamos, at DPG, and at APG. These locations were used to expand the variety of atmospheric conditions and aerosol loadings encountered. The results from these field tests were used to optimize the algorithm and investigate its sensitivity to the lidar operating parameters.

In the case of the tests at DPG, range anemometer data (15 minute averages) were used to indicate the general accuracy of the wind measurements. At APG our Army Research Laboratory colleagues provided a set of wind anemometers placed at 500, 700, 800, and 1000 m ranges. During the field test, several sets of wind measurements were undertaken simultaneously by both the lidar and the wind anemometers. We evaluated the accuracy and/or consistency of the wind measurements from the lidar using those obtained by the anemometers.

In Fig. 1 we plot the crosswind velocity measured by the lidar system as well as that obtained from the anemometers at 500 m range at APG. On the bottom half of the figure we plot the correlation magnitude. One immediately notices the one second fluctuations in the anemometer data. The correlation threshold, defined to mean the minimum correlation magnitude necessary for a "good" wind velocity measurement, was picked to be 0.17 in this case. For correlation thresholds less than 0.17, the previous wind velocity is assumed to still be in effect (but is degraded towards zero velocity by the algorithm) so that the fluctuations appear less rapid. We will indicate how important the choice of correlation threshold value is below.

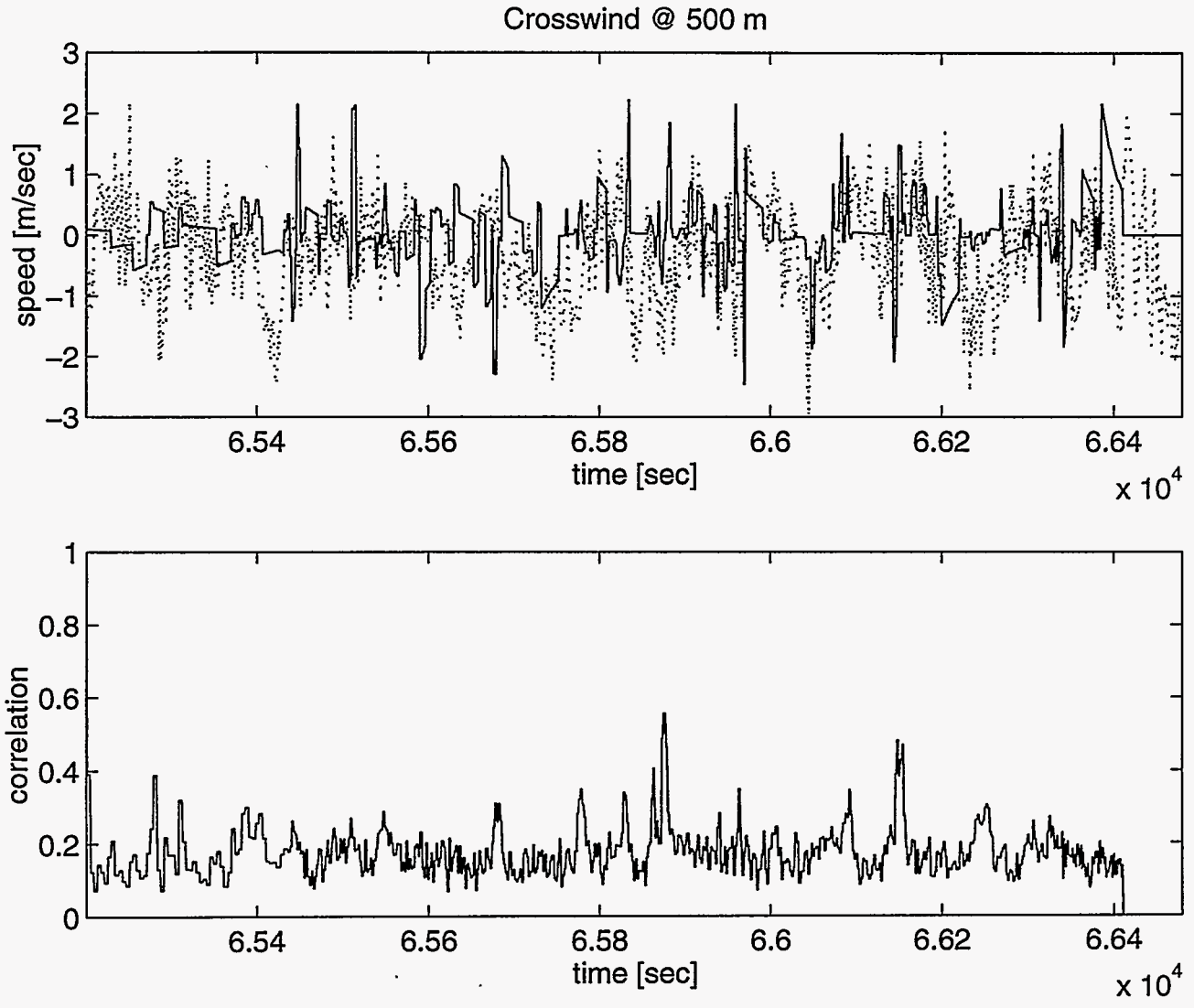

Fig. 1. (Top) Crosswind velocity measured by lidar system (solid line) and anemometer (dashed line) at 500 m range. (Bottom) Correlation magnitude. Data from tests at APG.

In Fig. 2 we plot the lidar system measured crosswind velocity at 400 m range at DPG during a series of experiments in which the atmosphere was artificially loaded with dust. The dust clouds can be seen in the correlation data at times of very large correlation values.

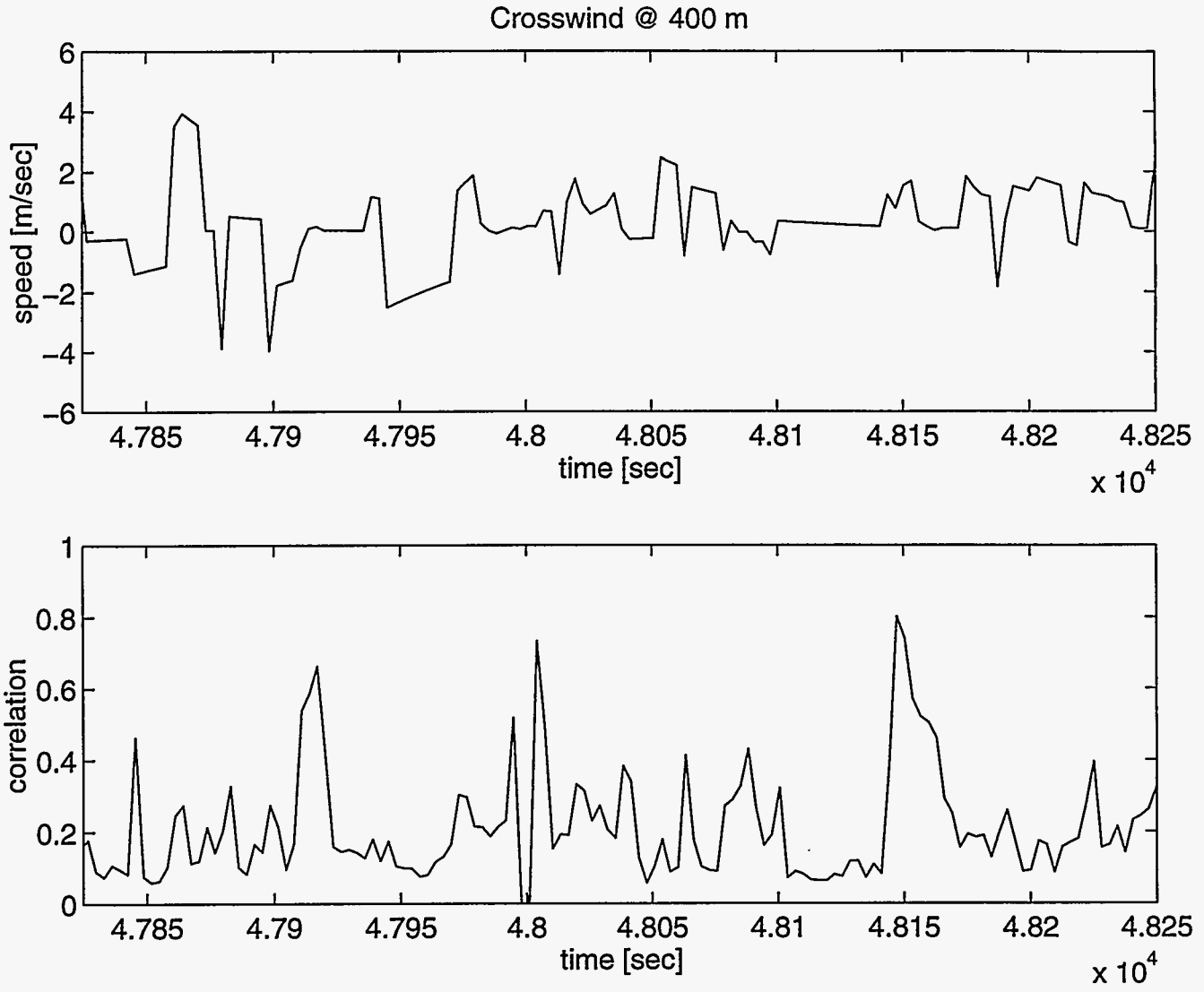

Fig. 2. (Top) Crosswind velocity at 400 m range measured at DPG by the lidar system. (Bottom) Correlation magnitude. Note large correlation values that occur during passage of dust clouds, corresponding to measured crosswind velocities consistent with DPG anemometers (see text).

4. CONCLUSIONS

The correlation threshold value of 0.17 was chosen using both the synthesized aerosol data and the archived data from field tests primarily at APG. The reason for this choice was to achieve a reasonable number of "good" wind velocity measurements (as the higher the threshold, the fewer number of scans result in an above-threshold correlation value). Lower thresholds caused wild fluctuations of the calculated wind velocity in some data sets. Higher thresholds resulted in stagnant readings (i.e. the system appears to have a slow response time).

Use of a faster detector and digitizer should enable the lidar system to detect a larger number of aerosol structures of smaller size. Presumably, there would also be an increase in the number of structures that can be correlated, leading to higher correlation values. This improvement would also therefore enable a higher correlation threshold and lead to improved calculated wind velocities.

We believe the algorithm, even with histogram equalization and moving median filtering, remains somewhat sensitive to edge effects, wherein a feature recognized in one scan moves off the edge in the next scan and another feature starts to enter at the opposite edge. Some of the large calculated wind velocities apparent in Fig. 1 may be due to this cause.

We also believe that noise in the lidar data can sometimes cause the algorithm to return a large wind value, e.g. when the noise in the data from one scan happens to correlate with noise in a following scan. A higher correlation threshold value avoids this error, but in atmospheres with small amounts of aerosols, the correlations are usually quite small.

It was also observed that fluctuations of the lidar returns from "solid" objects (meaning tree branches in this case) can cause the algorithm to give spurious wind velocities. Normally, the signals from trees were off scale, which causes very little interference for the algorithm (it sees a bunch of zeros, essentially). Often, however, signals other than off scale were observed, which, because of leaf movement or something similar, jumped around chaotically from scan to scan. These chaotic movements sometimes led to spurious algorithm results, resulting in predictions of larger fluctuating winds. Solid immobile objects are ignored in the algorithm, but no facility was built in to account for signals from chaotic movements of solid objects.

In order to show that the algorithm works well and predicts sensible winds when the correlation values are reasonable, we analyzed the DPG data where we created artificial aerosols (dilute dust clouds). The fifteen minute averaged wind velocity from the meteorological towers close to the lidar installation indicated 5-8 knot winds from 160-200° (approximately left to right across the lidar scan). When the correlation values were above 0.3 (from the dust), the algorithm predicted 0-2 m/s left to right cross winds and 0-1 m/s downrange winds, in reasonable agreement with the anemometer data (see Fig. 2). Correlation values between 0.17 and ca. 0.3 sometimes resulted in spuriously large wind velocity predictions. We believe these results agree with the statement that the algorithm produces reliable wind velocities when enough aerosols as well as coherent enough aerosol patterns exist to produce correlation values above 0.3.

5. ACKNOWLEDGMENT

This work was performed under the auspices of the US Department of Energy and was funded by the US Special Operations Command (SOCOM) (Col.-ret. William Williams) via the US Army Command (AMCOM) (Steve Small). The authors are especially appreciative of the entire XM94 lidar team, including R. Kevin Grace, James Busse, Victor Romero, John Brucker, and John Sutton. We are indebted to our Army Research Laboratory Colleagues Raymond Von Wahlde and Tom Haug for their willingness to acquire and supply anemometer data for us.

6. REFERENCES

1. J.L. Schols and E.W. Eloranta, J. Geophys. Res. 97, 18 395- 18 407 (1992).

2. D.R. Miller, University of Connecticut, personal communication.

DISCLAIMER